

Non-linear Aspects of Friction Material Elastic Constants

Donald E. Yuhas

Industrial Measurement Systems, Inc.

Jim Ding and Srikanth Venkatesan

TMD Friction North American R & D Center

ABSTRACT

In this report, we describe the ultrasonic measurement process applied to a series of three brake pad materials with varying degrees of load-dependent, non-linear behavior. For each material type, we measure the spatial variation of the ultrasonic velocity and the spatial variation of ultrasonic attenuation on several, as-manufactured, brake pads. We correlate these ultrasonic test results with those obtained by conventional compressibility tests. Subsequently, we destructively analyze each friction material. The load-dependence of the through-the-thickness longitudinal and shear velocity is measured using static loads ranging from 0.5 MPa to 8.0 MPa. For selected friction materials exhibiting significant variations in velocity with load, we compute the full set of engineering constants. Our analysis includes computation of the Young's modulus, shear modulus, and Poisson's ratios as a function of load. We discuss the sensitivity and repeatability of the methods and their application to both material formulation development and improved material uniformity.

INTRODUCTION

The Noise, Vibration and Harshness (NVH) behavior of braking systems is a complex problem involving the simultaneous interaction of several materials and numerous systems design variables. Many developers of braking systems have resorted to modeling and simulation in an effort to understand the various factors that determine performance. As input to the noise and vibration models, accurate material property data such as the Young's modulus, shear modulus, and Poisson's ratio are essential. The determination of relevant elastic properties is challenging due to the use of several friction materials with material inhomogeneity, anisotropy, and non-linear properties.

Although significant progress has been made in both modeling and measurement methods, no single measurement or modeling approach is sufficiently robust

to permit *a priori* prediction of a friction material's performance in new braking applications. In this paper, we discuss the ultrasonic measurement of elastic constants with an emphasis on the role of spatial variations and non-linear, load-dependent material properties.

EXPERIMENTAL METHODS

The intent of this study is two-fold: 1) to use ultrasonic methods to carefully characterize the uniformity of as-manufactured brake pads and 2) to determine the influence of non-linear load-dependent properties on the measurement and computation of friction material engineering constants. In contrast to laboratory methods used in destructively measuring friction material elastic constants, in this study we placed a significant effort on non-destructively measuring the properties of as-manufactured pads in order to quantify the material variability.

Ultrasonic Methods

The use of ultrasound to determine the mechanical properties of materials is based on the fundamental relationship between the ultrasonic velocity and the material elastic constants. These methods have been described in a number of books and review articles.¹⁻⁵ A review article describing ultrasonic methods for measuring elastic constants of friction materials is given by Yuhas & Yuhas.⁶

The ultrasonic technique used in this study is an ultrasonic through thickness transmission technique. The basic concept of ultrasonic testing is illustrated in Figure 1. A short burst of high frequency sound (typically 1 MHz to 3 MHz) is generated from the transmitting transducer and propagates through the sample to the receiving transducer. Measurements are made of the transit time using the ultrasonic signal that is digitized at a rate of 50 MHz. Thus, a transit time precision of 20 nanoseconds can be achieved. If the thickness is

known, the ultrasonic velocity can be determined from the transit time measurement. By measuring velocities of shear and longitudinal wave modes for different sample orientations, the material elastic constants can be determined. In order to efficiently couple the ultrasound to the sample, a viscous liquid coupling gel is used.

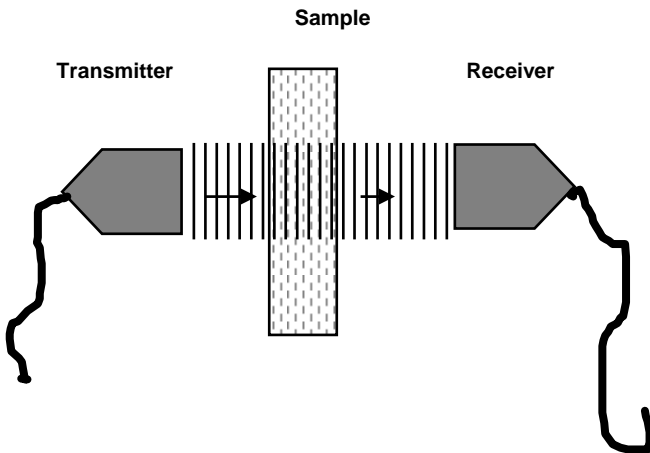


Figure 1 Basic ultrasonic data collection geometry.

In contrast to other measurements, (e.g. resonance or compressibility) ultrasonic velocity measurements are highly localized. This represents both one of the strengths and one of the weaknesses of this method. For inhomogeneous materials, it may be necessary to sample several areas in order to obtain a representative estimate of the pad properties. In contrast to previous ultrasonic studies where measurements were only made on friction material samples extracted from the intact brakes, in this report all samples were initially analyzed in the as-manufactured condition.

For our experiments, we use a 12.5 millimeter diameter transducer which defines the lateral extent of the probing field. For the longitudinal waves, data is taken using an ultrasonic frequency of 1 MHz. For shear waves we use a frequency of 2.25 MHz. All measurements are made in transmission so the beam interrogates the volume of the full thickness of the pad covered by the surface area of the transducer (1.22 sq. cm).

In addition to measuring the ultrasonic velocity, we also generated ultrasonic images of intact pads. For the images, only the signal loss is measured. Unlike the velocity, the signal loss is not fundamentally related to the elastic constants. However, the signal transmission is sensitive to local porosity, fiber/matrix bonding, and the bond integrity of the friction material/steel backing bond. For the ultrasonic images, the samples were immersed in a water bath which provided the coupling to the sample. This data provides a qualitative visual measure of material uniformity.

Compressibility

The compressibility of all pads investigated in this study was measured in accordance with SAE specification J2468. We report the absolute reduction in thickness for line pressure of 100 bar. All measurements were conducted at room temperature

SAMPLES

Three different passenger car brake pads were used for this investigation. The materials were chosen in order to obtain a range of nonlinear load dependent behavior. Our test set includes 2 high performance friction materials, HP-1 & HP-2, and one semi-metallic formulation SM-1. For each group, 6 pads were analyzed. The material formulation within each group is the same. However, HP-1 was sub-grouped into HP-1a and HP-1b. Although the friction formulation was the same within this group some aspects of the processing and the under-layer material differ. Each material group has a different pad geometry or “form factor”.

AS-MANUFACTURED “INTACT” PADS

Spatial Variation

In terms of their elastic properties, friction materials have transversely isotropic symmetry. Thus, in order to properly interpret the ultrasonic data, it is necessary to define a coordinate system relative to the brake pad. The coordinate system used for our study is illustrated in Figure 2 where the unique axis of our transversely isotropic solid is in the “3” direction (through-the-thickness). The friction materials are isotropic in the plane of the pad, “1” and “2” directions in Figure 2. This transverse isotropy is confirmed by the similarity of measured ultrasonic velocity for the in-plane longitudinal modes, $V_{11} = V_{22}$. For intact pads 4 velocity modes can be measured. This includes two in-plane modes V_{22} and V_{21} and two through-the-thickness modes V_{33} and V_{32} . In order to measure the uniformity of the pads we made multiple measurements of the V_{33} and V_{32} modes. The V_{33} mode is a longitudinal wave propagated through-the-thickness of the pad, while the V_{32} mode is a shear wave propagating through-the-thickness of the pad.

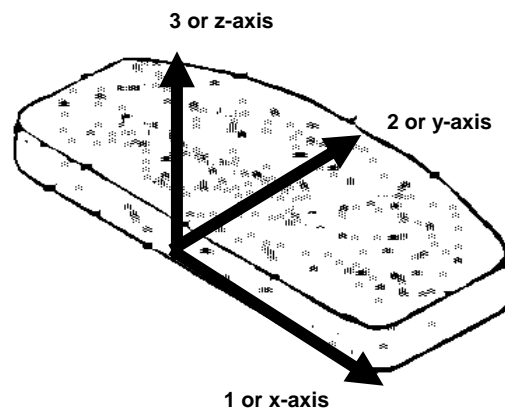


Figure 2 Coordinate definition referenced to a typical disk pad.

The V_{33} mode is related to the C_{33} diagonal element of the elastic constant matrix by the formula $C_{33} = \rho(V_{33})^2$ where ρ is the density. Thus, the value of V_{33} is related to the stiffness in the through-the-thickness, “3” direction. The V_{32} mode is a shear wave mode and is related to the C_{44} elastic constant by the formula $C_{44} = \rho(V_{32})^2$.

For each pad, multiple locations were measured. In some pads, seven measurements were made while in others only five measurements were made of each mode. In all cases, a force of 890 N (200 lbs) was used to couple the transducers to the friction material. A viscous, organic coupling compound, (IMS-SWC), was used to promote ultrasonic transmission.

In general, in order to make a meaningful measurement of the ultrasonic velocity, it is necessary to have flat and parallel entrance and exit areas for the ultrasonic beam. For those pads that have holes in the steel backing plate, it is necessary to avoid these zones and thus they are excluded from the measurement process.

The measurement process begins with generating a scanning template which is illustrated in Figure 3. In this case, we measure seven locations in each pad as indicated by the numbered circles in Figure 3. The smaller, shaded circles indicate the steel backing through holes. Each measurement area is 12.5 millimeters in diameter. As can be seen from the diagram, positions 1 and 7 represent the leading and trailing edges of the pad, positions 3, 4, and 5 are all located on the inner radius and the other positions 1, 2, 6, and 7 are on the outer pad radius.

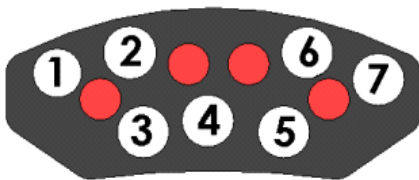


Figure 3 Template showing the backing plate through holes (red) and the measurement positions 1 through 7 for sample HP-1.

Figure 4 shows the measured V_{33} and V_{32} ultrasonic velocities on all seven positions of six HP-1 pads. In this case the six pads had identical construction or “form factors”. Even though the friction material formulation for this material group was similar, the under-layer and certain processing conditions differ so we have subdivided this group into two sub-groups labeled HP-1a and HP-1b. It is clear from Figure 4 that the properties measured for HP-1a differ from those measured for HP-1b, with HP-1b exhibiting lower average velocities for both V_{33} and V_{32} .

It should be noted here that even though the velocities have been measured by transmitting the ultrasound

through the steel backing, the influence of the steel backing is removed from the data. The values presented in Figure 4 (and throughout this paper) depend only on the friction material/under-layer properties. The correction factor for the steel backing is on the order of 20%. This may impart some systematic bias into the velocity data, but will not seriously impact the variability of the data. Relative to the friction material, the steel is uniform in both thickness and elastic properties.

The Figure 4 plots are intended to show both the pad-to-pad variations and the variation within each pad. Each plotted data point is the average value obtained from the 7 measurements on each pad. The error bar represents the standard deviation of the seven measurements. The variation in the former represents the pad to pad variations and the error bars on each point represent the variation in each pad.

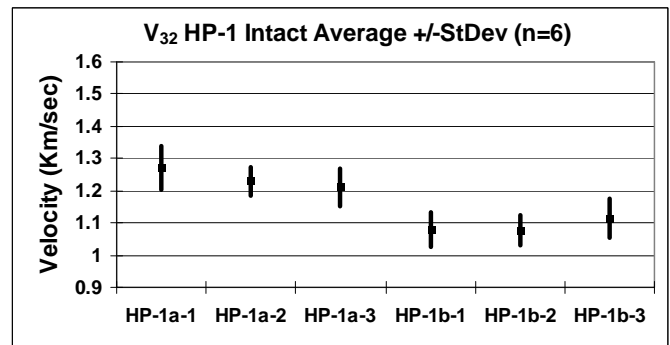
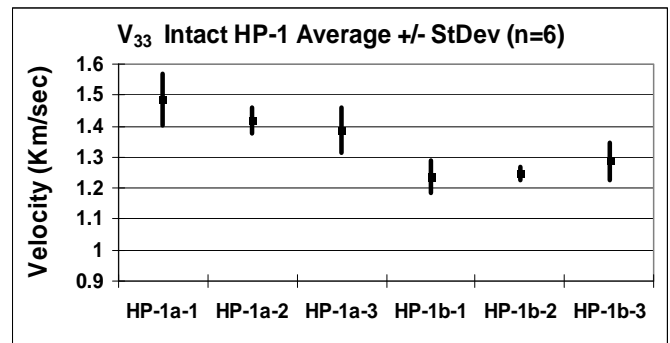


Figure 4 V_{33} and V_{32} measurement on 6 pads comprising material group HP-1.

It is also of interest to determine if there are any systematic spatial variations in the measured velocities that might be related to processing. To investigate this, we analyze HP-1a and HP-1b separately. The average value and standard deviation of the measured velocity for each position is computed. This data along with the measurement template is plotted in Figures 5 and 6. Figure 5 shows the data for sub-group HP-1a for both the V_{33} and V_{32} modes. Figure 6 shows the data for sub-group HP-1b for both the V_{33} and V_{32} modes.

There is a suggestion that the velocities measured near the pad center, #4, to be lower than those measured on the pad exterior e.g. #1 and #7. This trend is observed in

other samples analyzed in this study. This trend is more apparent for the shear mode V_{32} . Similar observations regarding the inner radius positions compared to the outer radius can also be made.

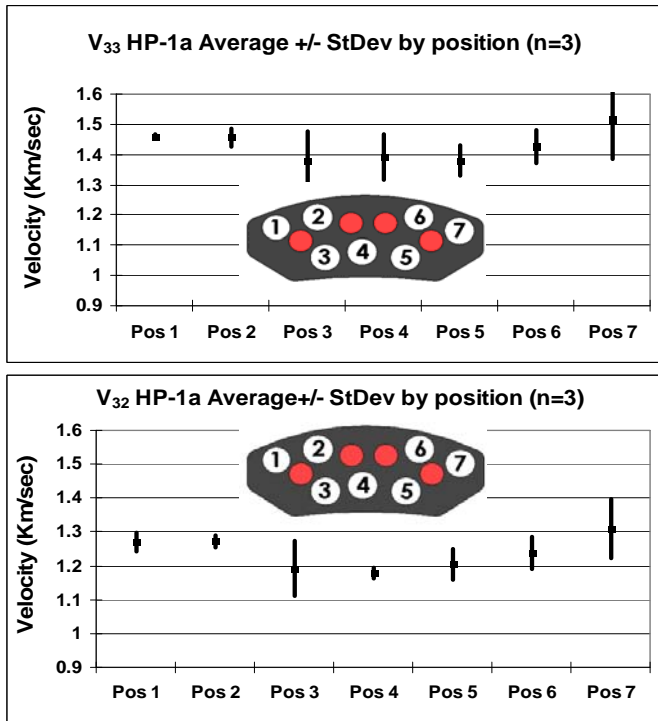


Figure 5 Spatial variations of V_{33} and V_{32} in 3 brake pads comprising sub-group HP-1a.

performance brake pads of group HP-2. These results are plotted in Figures 7 to 10. The average values and standard deviation for each pad of the semi-metallic material SM-1 is shown in Figure 7.

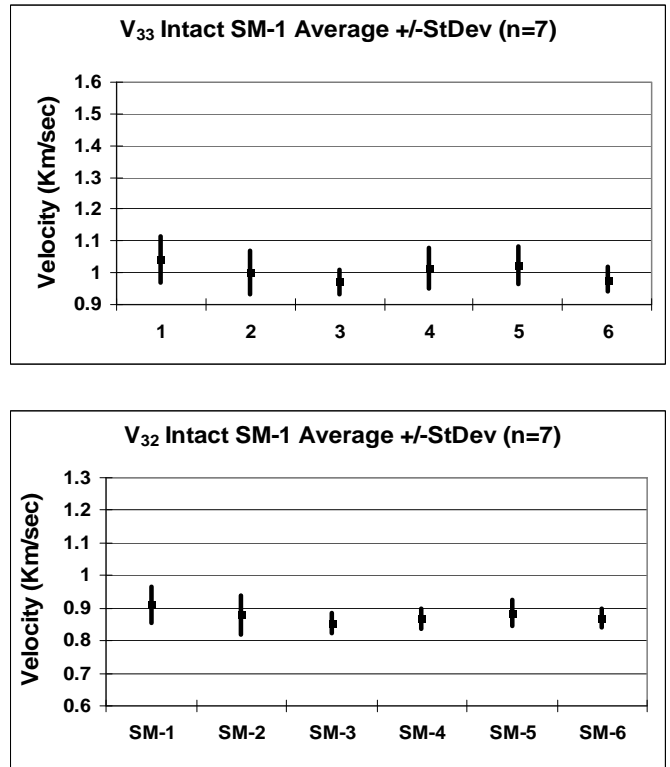


Figure 7 V_{33} and V_{32} measurement on the 6 brake pad of group SM-1.

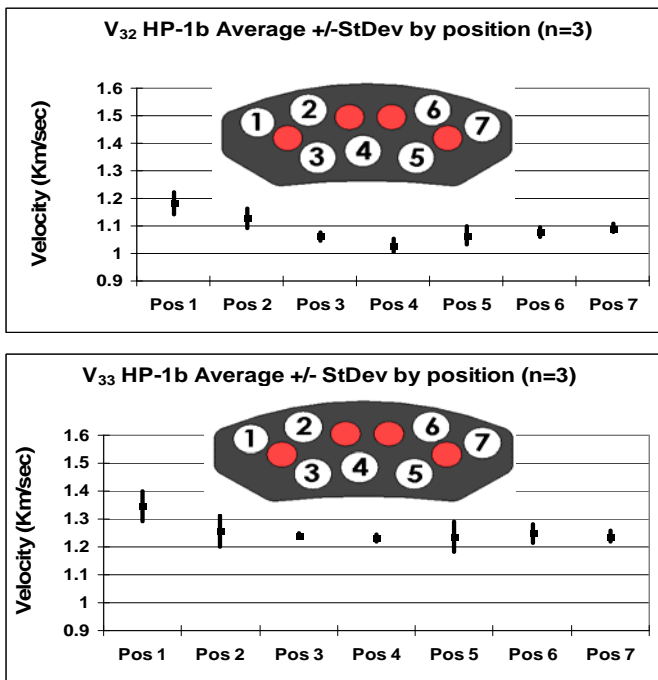


Figure 6 Spatial variations of V_{33} and V_{32} in 3 brake pads comprising sub-group HP-1b.

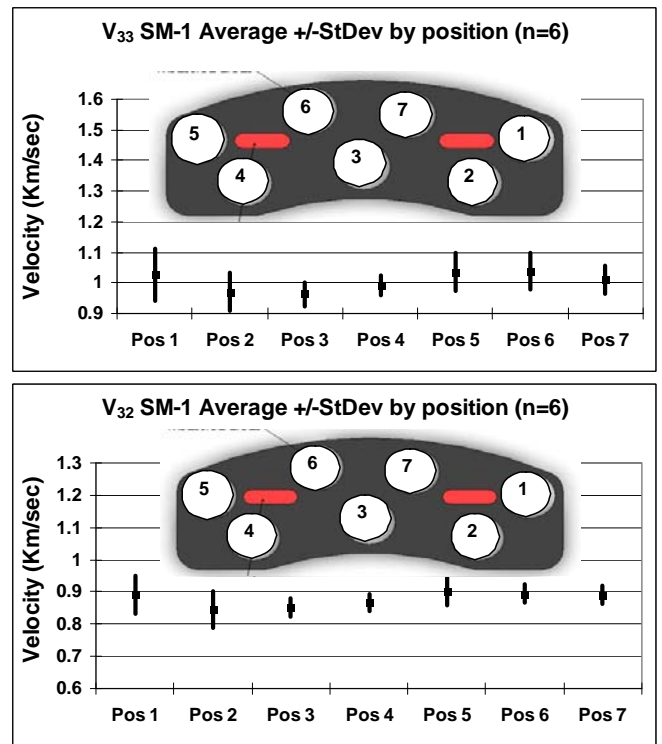


Figure 8 Spatial variations of V_{33} and V_{32} in 6 brake pads comprising group SM-1.

Comparable measurements have been made on six semi-metallic samples of group SM-1 and six high

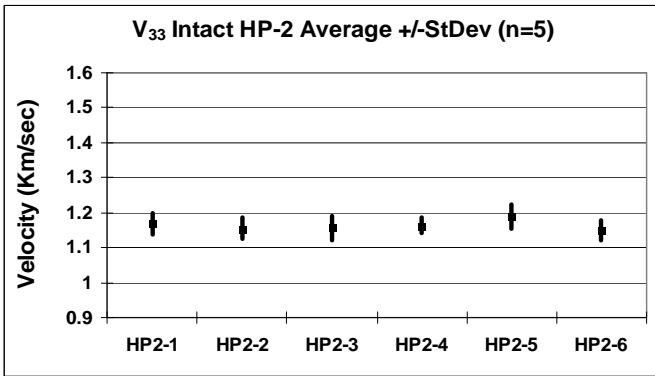
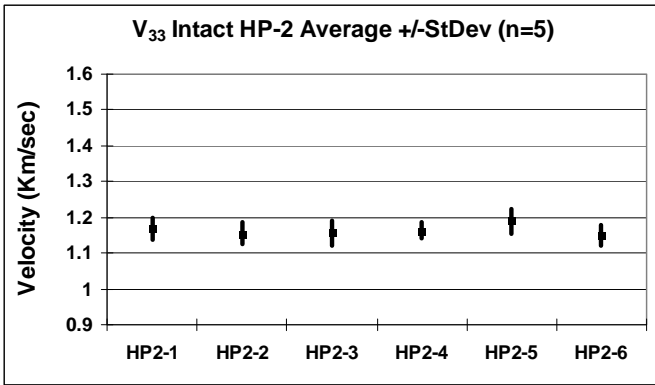


Figure 9 V_{33} and V_{32} measurements on 6 brake pads comprising group HP-2.

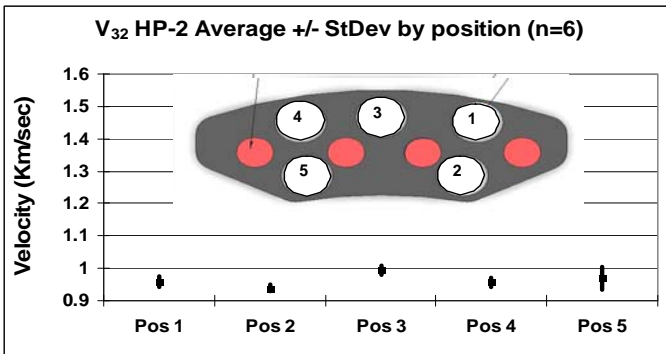
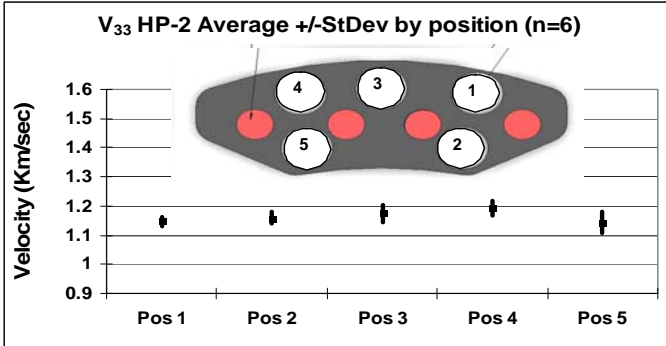


Figure 10 Spatial variations of V_{33} and V_{32} in the 6 brake pads comprising group HP-2

In this case, the sample to sample variations (average of the 6 points) appears to be less than the variation within a sample (the average of the error bars). Figure 8 shows the variation of velocity with position for the 6 samples of group SM-1. This graph shows a trend similar to that found in group HP-1. Specifically, there is a slight trend for the leading/trailing edge positions to have higher measured velocities relative to the interior. Note that in this case, the measurement template differs from that of HP-1. Here the leading and trailing edge positions are “1” and “5” while the center position is “3”.

The HP-2 material group is shown in Figure 9 and Figure 10. It is clear that this group show superior sample to sample uniformity as well as better uniformity within each sample compared to the other friction material groups.

Table I and Table II summarize the average and standard deviation of the measured velocities for the materials analyzed. Two standard deviations are listed. One, the group standard deviation, measures the sample to sample variability while the other, the sample standard deviation, measures the average variation within each sample. Both measures may be useful from a quality perspective. It is interesting to note that in most materials the variation observed in a single sample exceeds that observed between different samples. The magnitude of the variation is also quite large relative to the measurement precision which we estimate at +/- 0.3 %. For example, if similar ultrasonic measurements were carried out on a conventional engineering material e.g. steel, aluminum, plastic, both group and sample deviations would be on the order of 0.3 %. This is an order of magnitude lower than that observed on friction materials.

Table I Longitudinal Mode V_{33}

Mat'l Type	<Velocity> (Km/sec)	Group % STDev	#	Sample % STDev	#
HP-1a	1.43	4.65	3	4.91	7
HP-1b	1.257	2.13	3	3.53	7
HP-2	1.164	1.19	6	2.6	5
SM-1	1.005	2.66	6	5.71	7

Table II Shear Mode V_{32}

Mat'l Type	<Velocity> (Km/sec)	Group % STDev	#	Sample % STDev	#
HP-1a	1.237	4.62	3	3.07	7
HP-1b	1.091	1.87	3	4.88	7
HP-2	0.963	0.96	6	2.8	5
SM-1	0.878	2.13	6	4.64	7

ULTRASONIC IMAGES OF PADS

In addition to the velocity measurements made in each as-manufactured pad, we also produced ultrasonic images as an additional measure of pad spatial uniformity. Unlike the velocity measurements where we

have removed the influence of the steel backing member, the images include properties of the friction material, the under layer and the steel backing. At low Megahertz frequencies, the attenuation in the backing plate is negligible; however, there is a significant reflection at the steel/friction material interface due to the mismatch of acoustic impedance. Thus, the steel will contribute to the overall signal loss. The image spatial resolution is determined by the ultrasonic transducer operating frequency and physical size of the transducer. In this case, the resolution is on the order of 12 millimeters.

In order to image an intact pad, we use a through transmission geometry illustrated in Figure 11. In this case, the ultrasound is propagated through a conducting water path to allow for continuous scanning. Images are produced by mechanically scanning the transducer pair in a raster pattern with the sample “sandwiched” between the transducer pair. At each point in the scan, the amplitude of the transmitted wave is recorded and plotted. In theory, transit time (velocity) images can also be produced but this was not done in this study. The images are color-coded such that a region of high transmission appears red and regions of low transmission are coded in blue.

The display scheme has only a limited dynamic range so that system gain must be adjusted in order to achieve signal levels in the appropriate range for display. By tracking the system gain, we can obtain a relative measure of attenuation of the pads. For materials HP-1b, SM-1, and HP-2 the gain was set at 67 decibels while for HP-1a, a lower gain setting of 57 decibels was used. Higher gain settings indicate higher sample attenuation.

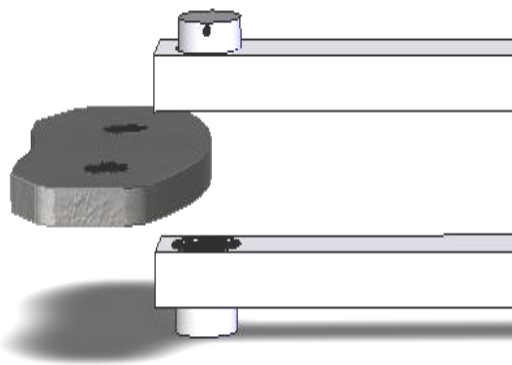


Figure 11 Through-the-thickness-transmission ultrasonic imaging geometry.

Representative ultrasonic amplitude images of intact pads from each material group analyzed previously are shown in Figure 12a, 12b, and 12c. Figure 12d shows an ultrasonic image obtained on a pad from group HP-1b after the steel backing and underlayer has been removed.

Figure 12a shows an image obtained on one pad from sub-group HP-1a obtained at a system gain of 57 decibels. Of all sample groups analyzed, this group shows the lowest attenuation (signal loss) but the highest attenuation variability. It should be noted that this group also exhibited the largest deviations in ultrasonic velocity.

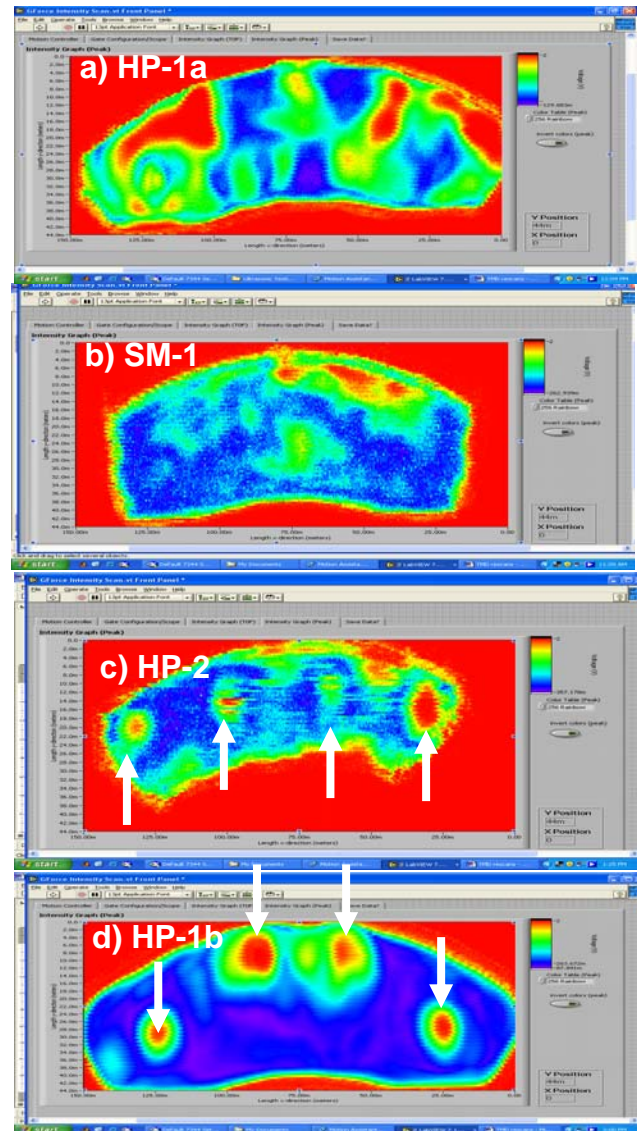


Figure 12 Representative ultrasonic Images of brake pads from each material group. a) Intact HP-1a; b) Intact SM-1; c) Intact HP-2 and d) sample HP-1b after removing the steel backing plate. Arrows indicate high transmission zones associated with region above the through-holes in the backing plate.

Figure 12b shows a representative image on a pad from group SM-1. This image shows a narrow region of increased transmission along the outer radius.

Figure 12c shows an image obtained on a sample from group HP-2. The steel backing on this pad had 4 through holes. Zones of increased ultrasonic transmission

associated with these through holes are indicated by arrows.

Figure 12d shows a representative image from group HP-1b. In this case the steel backing and underlayer has been removed. The four circular zones (arrows) of increased signal strength are related to the regions where there were through-holes in the steel backing. Otherwise, the friction material appears quite uniform.

VELOCITY/COMPRESSIBILITY CORRELATIONS

It is of interest to compare the average velocities measured in the as-manufactured pads with other measurements such as compressibility. The compressibility depends not only on the material physical properties but also on the shape and thickness of the brake pad. In contrast, ultrasonic velocity values are not dependent upon the dimensions of the pad. Thus, it is necessary to limit our correlation to brake pads that have the same "form factors".

In Figure 13 we show the correlations between the square of the velocities (V_{33} and V_{32}) with the deflection measured from a conventional compressibility test. Unfortunately, the correlations suffer from poor statistics because we are limited to making the correlations within each individual group (pads with the same thickness and shape).

For the HP-1 material Figure 13a the correlations are best with $R^2 = .87$ for the V_{32} , mode and $R^2 = .81$ for the V_{33} mode. In this group of materials there was a reasonably large variation in both the compressibility deflection and ultrasonic velocities. For the other groups the variation in materials properties within the group are less and the corresponding correlations are much poorer. In all cases the trend line is in the appropriate direction. Higher deflections are related to lower ultrasonic velocities (modulus). The correlations taken individually are not great but all relationships are consistent.

LOAD-DEPENDENT PROPERTIES

All previous data was collected using a coupling force of 200 pounds. Because the ultrasonic transducers were coupling the friction material on one side and the rigid steel backing plate on the other side, the loading pressure is complex but is on the order of 5 MPa. In this section, we will investigate the influence of load on the measured ultrasonic velocities.

For linear elastic materials, the measured ultrasonic velocity is independent of load. In general, load is applied only to achieve sufficient signal strength and to "squeeze" the coupling layer. This insures that the coupling layer is thin and, as a consequence, does not influence the transit time measurement used for the velocity determination. It has been found in some friction materials that the measured ultrasonic velocity is dependent on the load. It is apparent that for the proper

characterization of friction materials that the influence of load must be taken into account.

In order to make a measurement under load, a small compression test fixture is used to hold the ultrasonic sensors. The samples are sandwiched between the two transducers (~12 mm in diameter) and the transit time is measured as a function of load. Because the contact area is small (1.22 sq. cm), reasonably large pressures (8 MPa) can be generated with coupling forces of a few hundred pounds.

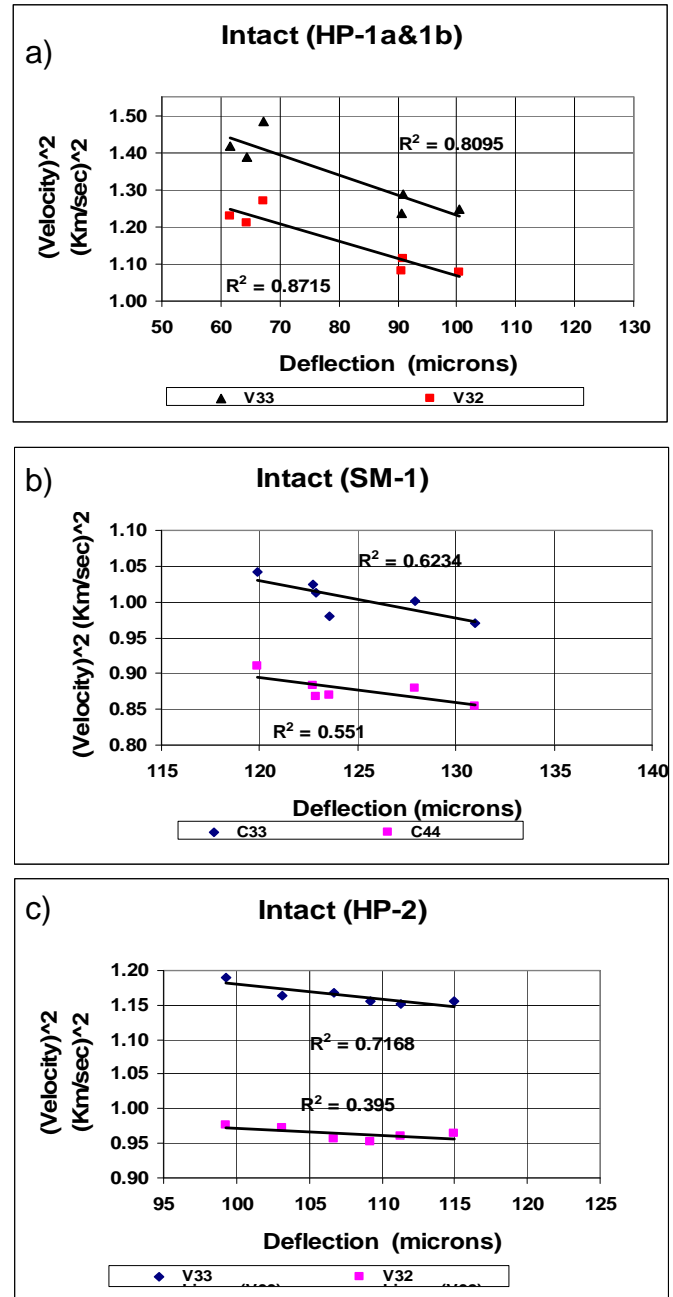


Figure 13 Correlation of Compressibility deflection with measured V_{33} and V_{32} a) HP-1 b) SM-1 c) HP-2

Before presenting the data obtained on friction material, we need to present data obtained on linear materials so

that we can validate the method and determine load sensitivity. Figure 14 shows data obtained on a Lexan plate using coupling pressures from 0.5 MPa to 8 MPa. We have chosen Lexan because it has a Young's modulus of 2.29 GPa which is comparable to that found in friction materials. We have plotted the percentage change in modulus (proportional to the measured velocity squared) as a function of coupling pressure. All data is normalized to the value obtained at the highest load. The results are plotted for the V_{33} mode ($C_{33} = \rho (V_{33})^2$) and the shear mode, V_{32} ($C_{44} = \rho (V_{32})^2$).

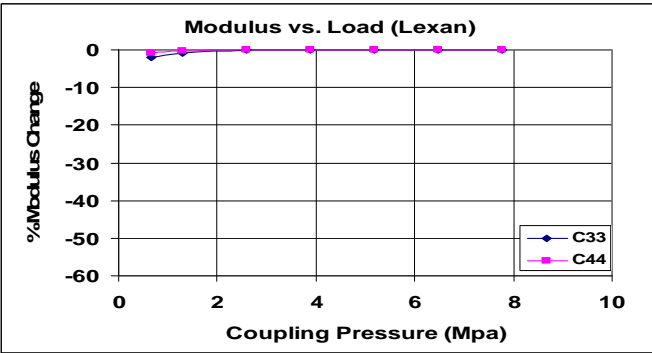


Figure 14 Load dependence of linear material

Contrast the results presented in Figure 14 with those shown in Figure 15 obtained on each friction materials group. This data was obtained on the same friction material samples previously analyzed after the steel backing member and the underlayer has been removed. As can be seen, the three groups vary considerably in their load-dependent response. The SM-1 material shows the least load dependence while the high performance material HP-2 exhibits considerable variation with load. In all cases, the variation in the shear modulus is less than that observed in the longitudinal modulus.

The data presented in Figure 15 is representative of the materials within each friction material group. Although these plots were obtained on single 1.22 sq. cm regions. A minimum of five regions on each pad were measured to insure the applicability of each curve in representing each group.

Clearly from a measurement perspective it would be desirable to measure the velocity at loads above 4 MPa where the variation with load is diminished. However, from a standpoint of modeling and simulation it may be desirable to measure the properties in the load range that they are subjected to during operation.

LOAD SENSITIVITY OF ENGINEERING CONSTANTS

It is of interest to determine the influence of load on the calculation of engineering constants from ultrasonic data. The results presented in the previous section show data obtained on only the through-the-thickness ultrasonic modes. These data suggest that there is considerable variation in the load dependence from one material to the next. This in itself might be useful for

characterizing the material. It certainly must be a factor in determining performance

In contrast to the variability in the through-the-thickness modes presented in the previous section, the in-plane modes are not load dependent⁶. This leads to several interesting features when one extracts engineering constants from the ultrasonic data.

For the intact (as-manufactured) pads, it is possible to measure 4 of the 5 independent velocities needed in order to calculate the engineering constants. Fortunately, the shear components appear as diagonal elements in the stiffness matrix and the extraction of the shear modulus is straight-forward. However, the Young's modulus and the Poisson's ratios are coupled. The complete set of velocity measurements are needed in order to complete the matrix inversion and calculate these engineering constants.

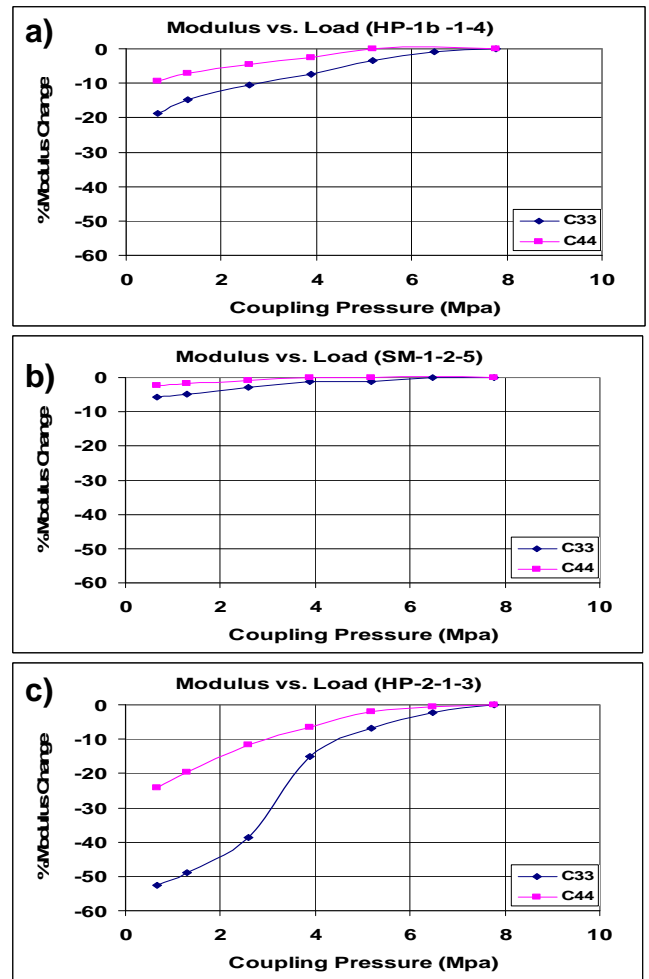


Figure 15 Typical load dependence of the shear (C_{44}) and the longitudinal (C_{33}) modulus for the 3 friction material groups a) HP-1; b) SM-1; c) HP-2.

The missing velocity value is derived from propagating a quasi-shear mode wave at 45 degrees relative to the unique, "3", axis⁶. This is routinely done in the laboratory

characterization of friction materials, but requires destructive analysis of the pad. It is instructive to investigate the sensitivity of the matrix inversion in that case where there is significant load dependence.

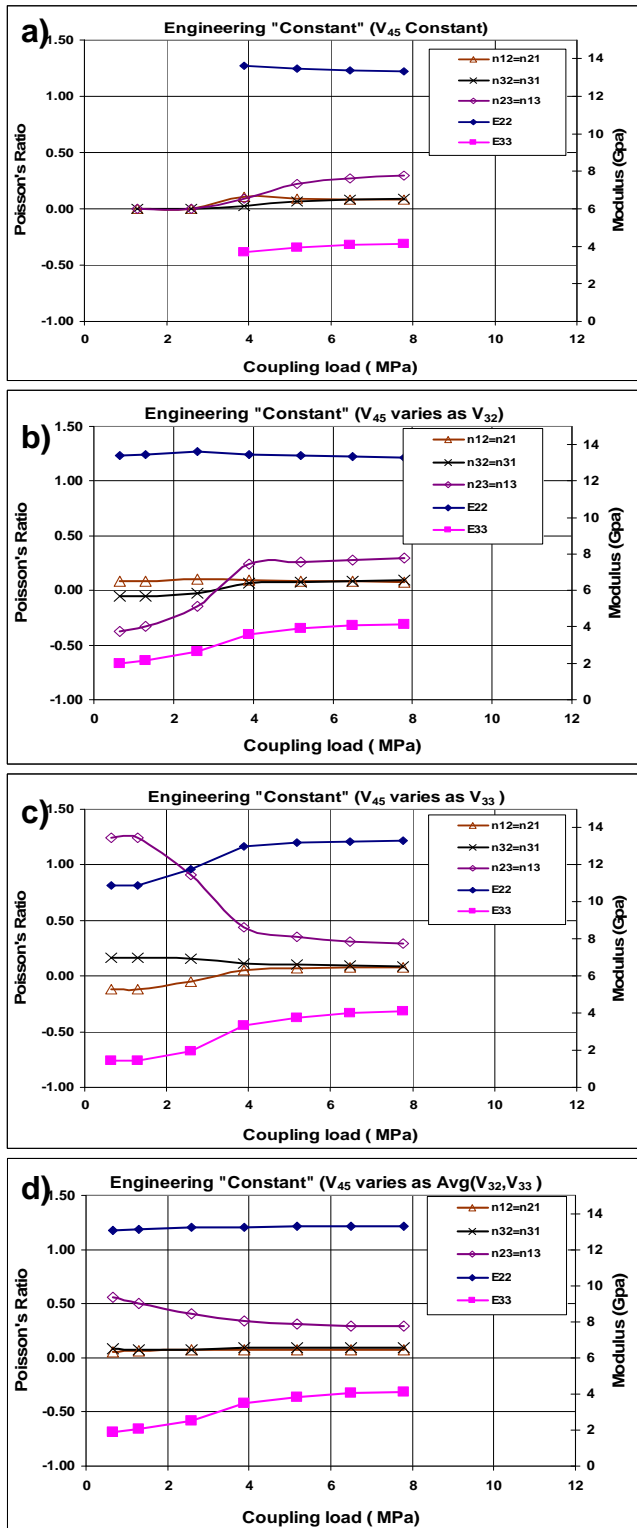


Figure 16 V_{45} mode model calculations of engineering constants (E_{22} , E_{33}) and Poisson's ratios (n_{12} , n_{32} , & n_{23}) for HP-2 friction.

To carry out this sensitivity analysis we use the four directly measured ultrasonic modes for the most load

sensitive material HP-2. This includes the velocity data shown in Figure 15c (V_{33} and V_{32}) and the non-load dependent in-plane modes V_{22} and V_{21} measured on the same pad. We parameterize the value and load dependence of the V_{45} mode. Four cases are considered: 1) no V_{45} load dependence; 2) V_{45} varies as V_{32} ; 3) V_{45} varies as V_{33} ; and 4) V_{45} varies as the average of V_{33} and V_{32} .

Figure 16 shows the results of model-dependent calculations of the in-plane Young's modulus, the through-the-thickness modulus, and the three relevant Poisson's ratios (n_{12} , n_{32} , and n_{23}) for HP-2 material. In Figure 16a we show the calculation for a V_{45} mode that has no load dependence. For loads below 4 MPa the matrix inversion results in indeterminate values for the in-plane Young's modulus E_{22} and the through-the-thickness modulus E_{33} . In Figure 16b we impart on the V_{45} mode the same load dependence as the V_{32} (Figure 15c) while for Figure 16c with impart on V_{45} the load dependence of V_{33} . Although the moduli are reasonably well-behaved, the Poisson's ratios take on unusual values.

Figure 16d shows the calculations where the load dependence of V_{45} is the average of the V_{33} and V_{32} . In this case both the modulus and Poisson's ratios are well-behaved. These results suggest that even though the modulus values are well behaved for the various loading models, the Poisson's ratios are quite sensitive.

DISCUSSION & CONCLUSION

In this report, we have presented for the first time quantitative measurements of ultrasonic velocity in intact, as-manufactured, automotive disc brake pads. Both longitudinal and shear modes have been non-destructively measured in the through-the-thickness direction. Multiple measurements have been made in each pad so that we not only measure the "pad average" but also the spatial variation of ultrasonic velocity within the pad. The influence of the steel backing has been removed from the data. Thus the ultrasonic data depends only upon the properties of the friction material and under-layer.

Results obtained on three friction materials show that the magnitude of the through-the-thickness ultrasonic velocity varies significantly both within a sample and from one sample to the next. For one material type, SM-1, variations (within a single sample) of more than 5 percent has been observed. Because the underlying elastic constants have a quadratic dependence on the velocity, this implies more than 10% variation in elastic properties.

We also present the first ultrasonic images on intact, as-manufactured brake pads. These images can be used to measure pad spatial uniformity. Although, care must be taken in interpreting these images, as multiple factors can influence the character of the images, they are useful for material characterization in the laboratory.

The current imaging method is too slow to be used as a quality assurance tool. However, incorporation of multi-element sensor arrays can be used to speed data collection and thus extend the technique to process control applications.

The correlation of the measured ultrasonic velocities with compressibility looks encouraging. Because of the in-pad variability cited above, it is important to make multiple measurements in order to obtain a representative pad average. As there is a fundamental relation between the measured velocities and elastic properties, we should anticipate a reasonable correlation with other methods that depend on mechanical properties. Correlations were only carried out within each brake pad group. This limited the sample size as well as the range of variation over which the results could be correlated. Further work is needed to extend comparisons to pads with differing "form factors".

The non-linear nature of friction materials has also been investigated. Data has also been presented showing the dependence of the through-the-thickness ultrasonic velocity measurements on load. The elastic constant, C_{33} , derived from the through-the thickness velocity, has been observed to vary by as much as 60 % for loadings ranging from 0.5 MPa to 8.0 MPa. For all materials investigated, we find that the load dependent variations in shear modulus, C_{44} are less than those measured for the longitudinal modulus, C_{33} . The three material groups analyzed differ significantly in their load-dependent behavior. We suggest that quantifying this non-linear behavior might be a valuable characterization tool.

Model calculations of the engineering constants and Poisson's ratios are used to investigate the combined effects of load dependence and anisotropic materials properties. It should be kept in mind that even though the through-the-thickness modes exhibit significant load dependence, the in-plane modes show little or no load dependence⁶.

For HP-2 friction material, the most load-sensitive material studied, our results show that for loads greater than 4 MPa, the Young's modulus, E_{33} and E_{22} and the three Poisson's ratios are relatively independent of the loading model. However, below 4 MPa, the results are sensitive to the load dependence of the V_{45} velocity. Although the Young's modulus, E_{22} and E_{33} always appear to be well behaved, the calculated Poisson's ratios vary wildly yielding unphysical (although allowable using the laws of physics) values.

Several of the above cited factors can combine to produce significant variability in engineering constants and Poisson's ratios derived from ultrasonic data. Spatial non-uniformity of velocities measured within individual pads can be a significant source of error. The large load-sensitivity of some friction materials requires that load be monitored and incorporated into the measurement process. Lastly, the large variation in Poisson's can be partly attributed to the matrix inversion

process which calculates the Poisson's ratios. A small variation in the elasticity matrix can result in large variation in engineering constants if the values are near singularities. Adequate sampling and monitoring of loads are essential for reliable ultrasonic measurements of elastic constants.

ACKNOWLEDGMENTS

We would like to express our appreciation to Dr. Marjorie P. Yuhas for many helpful discussions and Ms. Carol Vorres and Ms. Loretta Oleksak for their help in collecting data and generating graphics for this manuscript.

REFERENCES

1. Schreiber, E., Anderson, O.L. and Soga, M., Elastic Constants and Their Measurement, McGraw-Hill, New York, 1973
2. Truell, R., Elbaum, C. and Chick, B.B., Ultrasonic Methods in Solid State Physics, Academic, New York, 1969.
3. Thurston, R.N., in Physical Acoustics vol 1 eds. W.P. Mason and R.N. Thurston, Academic Press, New York, 1964.
4. Every, A.G. and McCurdy, A.K., Landolt-Bornstein New Series Group II, vol. 29a. ed. Madelung, Springer, Berlin, 1992.
5. Every A.G., "Determination of the Elastic Constants of Anisotropic Solids", NDT International Vol. 27, No. 1, p. 3, 1993.
6. Yuhas D.E. and Yuhas M.P. "Friction Material Elastic Constant Measurements" In Disc Brake Squeal- Mechanism, Analysis, Evaluation, and Reduction, eds. R.L. Quaglia, C.A. Tan and F. Chen, SAE December, 2005.

CONTACT

Donald E. Yuhas Ph.D

Dyuhas@imsysinc.com